Modeling Neural Mechanisms for Genesis of Respiratory Rhythm and Pattern. III. Comparison of Model Performances During Afferent Nerve Stimulation

ILYA A. RYBAK, JULIAN F. R. PATON, AND JAMES S. SCHWABER
Central Research Department, DuPont Experimental Station E-328/B31, Wilmington, Delaware 19880-0328; and Department of Physiology, School of Medical Sciences, University of Bristol, Bristol BS8 1TD, United Kingdom

Rybak, Ilya A., Julian F. R. Paton, and James S. Schwaber. Modeling neural mechanisms for genesis of respiratory rhythm and pattern. III. Comparison of model performances during afferent nerve stimulation. *J. Neurophysiol.* 77: 2027–2039, 1997. The goal of the present study was to evaluate the relative plausibility of the models of the central respiratory pattern generator (CRPG) proposed in our previous paper. To test the models, we compared changes in generated patterns with the experimentally observed alterations of the respiratory pattern induced by various stimuli applied to superior laryngeal (SLN), vagus and carotid sinus (CS) nerves. In all models, short-duration SLN simulation caused phase-resetting behavior consistent with experimental data. Relatively weak sustained SLN stimulation elicited a two-phase rhythm comprising inspiration and postinspiration whereas a stronger stimulation stopped oscillations in the postinspiratory phase (''postinspiratory apnea''). In all models, sustained vagus nerve stimulation produced postinspiratory apnea. A short vagal stimulus delivered during inspiration terminated this phase. The threshold for inspiratory termination decreased during the course of the inspiratory phase. The effects of short-duration vagal stimulation applied during expiration were different in different models. In model 1, stimuli delivered in the postinspiratory phase prolonged expiration whereas the late expiratory phase was insensitive to vagal stimulation. No insensitive period was found in model 2 because vagal stimuli delivered at any time during expiration prolonged this phase. Model 3 demonstrated a short period insensitive to vagal stimulation at the very end of expiration. When phasic CS nerve stimulation was applied during inspiration or the first half of expiration, the performances of all models were similar and consistent with experimental data: stimuli delivered at the beginning inspiration shortened this phase whereas stimuli applied in the middle or at the end of inspiration prolonged it and stimuli delivered in the first half of expiration prolonged the expiratory interval. Behavior of the models were different when CS stimuli were delivered during the late expiratory phase. In model 1, these stimuli were ineffective or shortened expiration initiating the next inspiration. Alternatively, in models 2 and 3, they caused a prolongation of expiration. Although all CRPG models demonstrated a number of plausible alterations in the respiratory pattern elicited by afferent nerve stimulation, the behavior of model 1 was most consistent with experimental data. Taking into account differences in the model architectures and employed neural mechanisms, we suggest that the concept of respiratory rhythmogenesis based on the essential role of postinspiratory neurons is more plausible than the concept employing specific functional properties of decrementing expiratory (dec-E) neurons and that the ramp firing pattern of the late expiratory neuron is more likely to reflect intrinsic properties than disinhibition from the dec-E neurons.

INTRODUCTION

This paper is the third in a series of papers presenting our efforts to investigate mechanisms for respiratory rhythm and pattern generation at the cellular, network, and system levels using modeling methods. The previous papers described models of single respiratory neurons (Rybak et al. 1997a) and two- and three-phase network models of the central respiratory pattern generator (CRPG) (Rybak et al. 1997b). The differences between the CRPG models included: the mechanism providing ramp firing patterns of late expiratory (E2) neurons; the functional roles of postinspiratory (post-I) and decrementing expiratory (dec-E) neurons, and the mechanism for expiratory termination. All CRPG models were tested previously under normal conditions and demonstrated both a stable respiratory rhythm and physiologically plausible membrane trajectories of respiratory neurons (Rybak et al. 1997b). In the present paper, we analyze model performances during stimulation of the superior laryngeal (SLN), vagus and carotid sinus (CS) nerves and compare the resultant behavior of the models with data obtained from in vivo experiments (Boyd and Maaske 1939; Bradley 1976; Clark and von Euler 1972; Cohen 1979; Eldridge 1972, 1976; Feldman 1986; Feldman and Gautier 1976; Gautier et al. 1981; Knox 1973; Larrabee and Hodes 1948; Lawson 1981; Paydarfar et al. 1986; Remmers et al. 1986; Richter et al. 1986; von Euler 1986; Younes and Polacheck 1981). The results of simulations have permitted comparative evaluation of our CRPG models.

METHODS

CRPG models

The present paper focuses on our three-phase CRPG models (3-phase models 1–3 in Rybak et al. 1997b). Analysis showed that the behavior of the our two-phase models (2-phase models 1 and 2; Rybak et al. 1997b) was similar to the behavior of three-phase model 2 during all types of stimulation used in this study. Thus although the two-phase models are not presented in this paper, all conclusions drawn here about three-phase model 2 are relevant to both the two-phase models as well.

Schematics of CRPG models 1–3 examined here are shown in Figs. 1*A* and 2, *A* and *B*, respectively. The weights of synaptic connections in the models are presented in Tables 1–3. Each model consisted of a network of synaptically interconnected respiratory neurons [early inspiratory (early-I); ramp inspiratory (ramp-I); late inspiratory (late-I); decrementing expiratory (dec-E); postin-

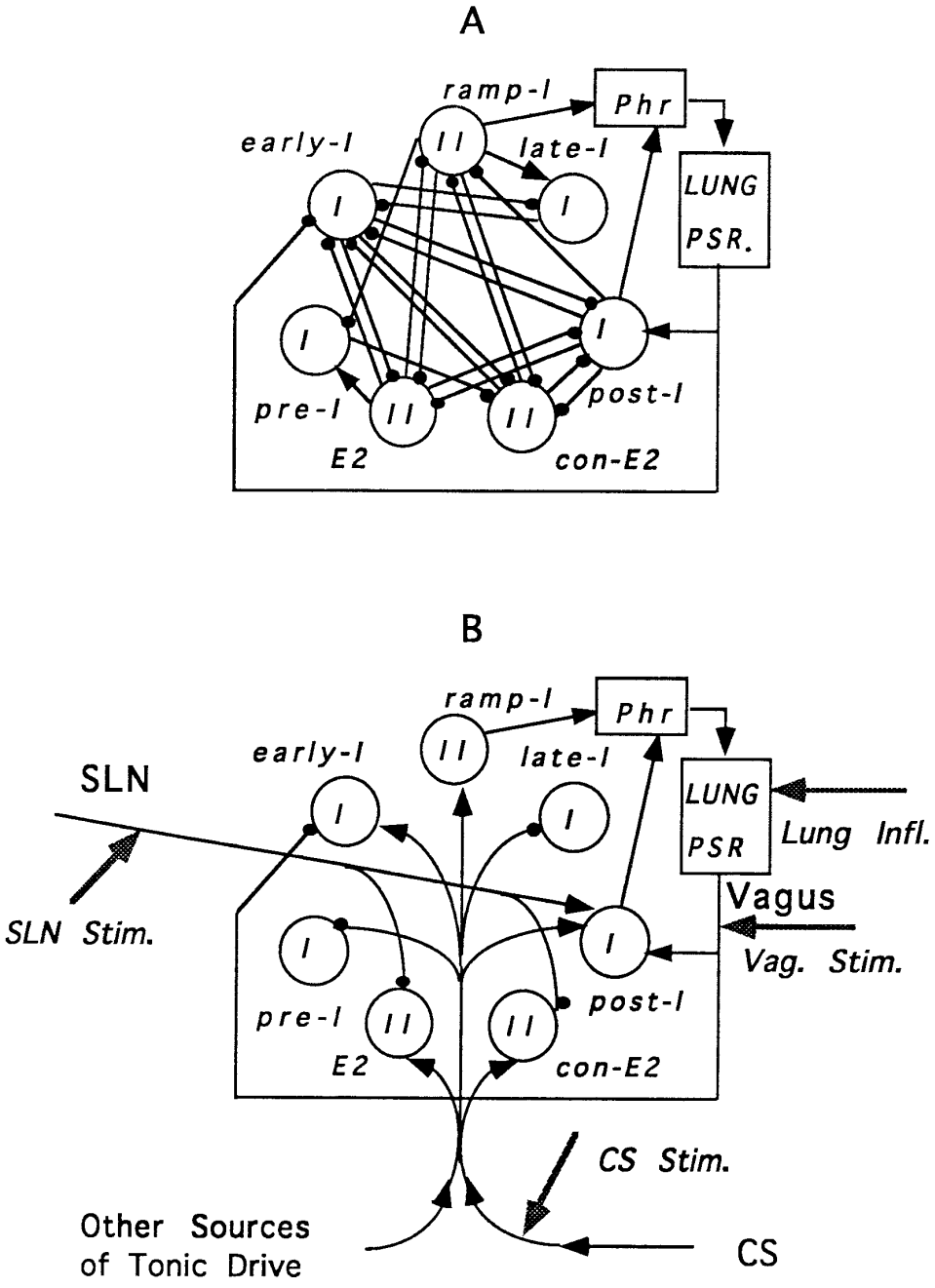

FIG. 1. Schematic of model 1. *A*: synaptic connections between the respiratory neurons; *B*: afferent inputs from peripheral nerves. Large circles represent neurons. Numbers inside circles indicate neuron types. Filled circle, inhibitory synapses; arrow, excitatory synapses. Large stippled arrows indicate points to which stimuli were applied in different model experiments.

spiratory (post-I); stage II expiratory (E2); stage II constant firing expiratory (con-E2); preinspiratory (pre-I)] and simplified models of lung and pulmonary stretch receptors (PSR). The integrated phrenic (Phr.) activity, considered to be the network output, was derived by weighted integration of ramp-I and post-I neuronal activities. The PSR provided feedback to the respiratory network via the vagus nerve.

Performances of CRPG models 1–3 under normal conditions are shown in Fig. 3, *A–C*, respectively. Each model generates a respiratory rhythm showing realistic discharge patterns of respiratory neurons. The mechanism for the inspiratory off-switch (switch between the inspiratory and postinspiratory phases) is the same in all models and operates via the late-I neuron, which is considered to be a switching neuron (Cohen 1979; Cohen and Feldman 1977; Feldman 1986). The mechanisms used for the expiratory off-switch operates via the pre-I neuron, which also acts as a switching neuron (Richter 1996).

The models studied differ by the following: the mechanism used to shape the ramp firing pattern of the late (stage II) expiratory (E2) neurons, the roles of post-I and dec-E neurons in the CRPG performance, and the mechanism used for termination of expiration. In model 1 (Figs. 1*A* and 3*A*), the ramp firing patterns of E2 neuron is based on its intrinsic properties (Rybak et al. 1997a). The post-I neuron is a key element in this model. It inhibits inspiratory neurons during the postinspiratory phase. In addition, its adaptive properties and reciprocal inhibitory interactions with the con-E2 and E2 neurons define the duration of the postinspiratory phase. During the late (stage II) expiration, the early-I neuron is inhibited by both the E2 and con-E2 neurons. The expiratory off-switch in this model operates in following way. The pre-I neuron, excited

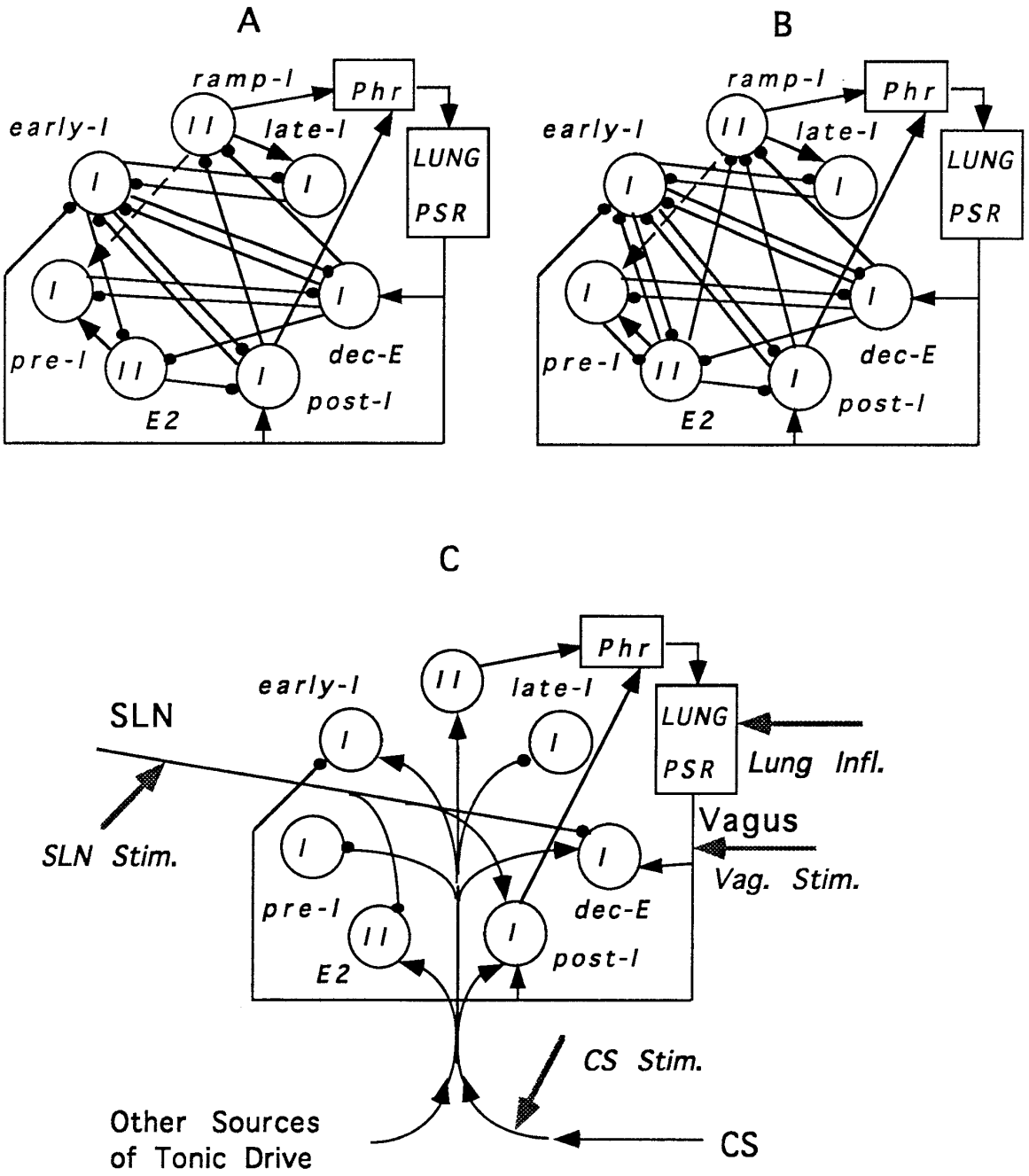

FIG. 2. Schematics of models 2 and 3. *A* and *B* represent synaptic connections between respiratory neurons in models 2 and 3, respectively. *C*: afferent inputs from afferent nerves in both models. Large circles represent neurons; numbers inside circles indicate neuron types. Filled circle, inhibitory synapses; arrow, excitatory synapses. Large stippled arrows indicate points of stimulation in different model experiments.

by the E2 ramp firing pattern, inhibits the con-E2 neuron (Figs. 1*A* and 3*A*). Termination of the con-E2 neuron activity leads to disinhibition of the early-I neuron, which initiates inspiration.

Unlike model 1, the ramp firing pattern of the E2 neuron in model 2 is based on disinhibition from the slowly adapting dec-E neuron (Figs. 2*A* and 3*B*). The dec-E neuron plays a much more important role in this model than the post-I neuron. The expiratory off-switch mechanism in model 2 also operates via the pre-I neuron, which is excited by the increasing activity of the E2 neuron. However, during the late (stage II) expiratory phase both early-I and ramp-I neurons are inhibited by the dec-E neuron (instead of E2 and con-E2 in model 1). Accordingly, the pre-I neuron in model 2 inhibits the dec-E neuron instead of the con-E2 neuron as in model 1. Cessation of dec-E firing disinhibits both inspiratory neurons and initiates inspiration.

Because disinhibition from the adapting dec-E neuron completely defines the ramp firing pattern of the E2 neuron (which, in turn, controls the timing of expiratory termination via the pre-I neuron), the dec-E actually controls the expiratory off-switching. This makes the behavior of this model similar to the behavior of both our two-phase CRPG models (Rybak et al. 1997b).

Model 3 combines the properties of both the above models (Figs. 2*B* and 3*C*). Like model 2, the ramp firing pattern of the E2 neuron in model 3 is based on disinhibition from the slowly adapting dec-

TABLE 1. *Model 1: types of neurons and weights of synaptic inputs*

Neuron	Type	Synaptic Weights of Inputs From Other Neurons W_{ij}							Tonic (including CS) W_{oi}	CS Percent in Tonic	Vagus W_{PSRi}	SLN W_{SLNi}
		early-I	ramp-I	late-I	post-I	con-E2	E2	pre-I				
early-I	I			−0.15	−0.45	−0.32	−0.15		+1.00	60	−0.02	
ramp-I	II				−2.00	−2.00	−2.00		+1.00	80		
late-I	I	−0.60	+2.40						−0.50	10		
post-I	I	−4.20				−0.28	−0.09		+1.00	50	+0.80	+0.1
con-E2	II	−2.80	−0.07		−0.40			−0.80	+1.00	30		−0.5
E2	II	−2.80	−0.07		−3.70				+1.00	30		−0.5
pre-I	I		−0.05				+1.93		−0.50	10		

Neuron types are early-I, early inspiratory; ramp-I, ramp inspiratory; late-I, late inspiratory; post-I, postinspiratory; con-E2, stage II constant firing expiratory; E2, late (stage II) expiratory; pre-I, preinspiratory.

TABLE 2. *Model 2: types of neurons and weights of synaptic inputs*

Neuron	Type	Synaptic Weights of Inputs From Other Neurons W_{ij}							Tonic (including CS) W_{oi}	CS Percent in Tonic	Vagus W_{PSRi}	SLN W_{SLNi}
		early-I	ramp-I	late-I	post-I	con-E2	E2	pre-I				
early-I	I			−0.15	−1.80	−0.45			+1.00	60	−0.02	
ramp-I	II				−4.00	−3.50			+0.90	80		
late-I	I	−0.60	+2.45						−0.50	10		
dec-E	I	−4.40						−0.30	+1.25	60	+0.56	−0.5
post-I	I	−3.40					−0.70		+1.00	60	+0.40	+0.1
E2	II	−3.50			−0.23				+1.00	30		−0.5
pre-I	I		+0.40		−0.25		+2.95		−0.50	10		

dec-E, decrementing expiratory.

TABLE 3. *Model 3: types of neurons and weights of synaptic inputs*

Neuron	Type	Synaptic Weights of Inputs From Other Neurons W_{ij}							Tonic (including CS) W_{oi}	CS Percent in Tonic	Vagus W_{PSRi}	SLN W_{SLNi}
		early-I	ramp-I	late-I	post-I	con-E2	E2	pre-I				
early-I	I			−0.15	−0.40	−0.45	−0.50		+1.00	60	−0.02	
ramp-I	II				−4.00	−3.20	−3.00		+0.90	80		
late-I	I	−0.60	+2.45						−0.50	10		
dec-E	I	−3.40						−0.50	+1.25	70	+0.56	−0.5
post-I	I	−2.40					−1.00		+1.00	60	+0.40	+0.1
E2	II	−2.50			−0.23			−0.45	+1.00	20		−0.5
pre-I	I		+0.42		−0.15		+3.00		−0.50	10		

E neuron. However, during the late expiratory phase, the early-I and ramp-I neurons are inhibited by both dec-E and E2 neurons (Figs. 2*B* and 3*C*). Correspondingly, to terminate expiration, the pre-I neuron inhibits both dec-E and E2 neurons.

Vagus nerve input to the respiratory network

It is known that PSR afferents do not innervate the respiratory neurons directly, but influence the central respiratory generator via an intermediate network of neurons (Cohen 1979; Feldman 1986; von Euler 1986). However, in this study, we have accepted the simplification used in earlier models (Botros and Bruce 1990; Geman and Miller 1976) in which the vagus nerve provides direct inputs to respiratory neurons. In all our CRPG models, PSR afferents inhibited the early-I neurons and excited the post-I (and dec-E in models 2 and 3) neurons (Figs. 1 and 2). The inhibitory inputs to early-I neurons are supported by the observation that these neurons are inhibited by lung inflation (von Euler 1986). Excitatory inputs to post-I neurons are based on the finding of excitation of post-I neurons after electrical stimulation of the vagus nerve (Remmers et al. 1986; Richter et al. 1987; von Euler 1986). The excitatory inputs to dec-E neurons are based on data that these neurons are excited by lung inflation (Cohen 1979; Ezure 1990; Feldman 1986).

The synaptic weights of PSR inputs to the above neurons used in models 1–3 are presented in Tables 1–3, respectively.

Tonic drive and CS nerve input to the respiratory network

It generally is accepted that neurons participating in the central respiratory pattern generation receive a tonic drive. This drive comes from different medullary (e.g., reticular activating system) and supramedullary (e.g., pons, hypothalamus) sources and central and peripheral chemoreceptors (Cohen 1979; Feldman 1986; Richter et al. 1986; von Euler 1986). Inputs from the peripheral chemoreceptors relay to the central respiratory generator in the CS nerve and are a part of the tonic drive. In our models, all types of respiratory neurons receive excitatory synaptic drive except late-I and pre-I neurons (Figs. 1*B* and 2*C*). The two latter neurons receive tonic inhibitory inputs. The inhibitory effects of peripheral chemoreceptors on late-I neurons are supported by experimental evidence (Lawson et al. 1989). Because no information on tonic (excitatory

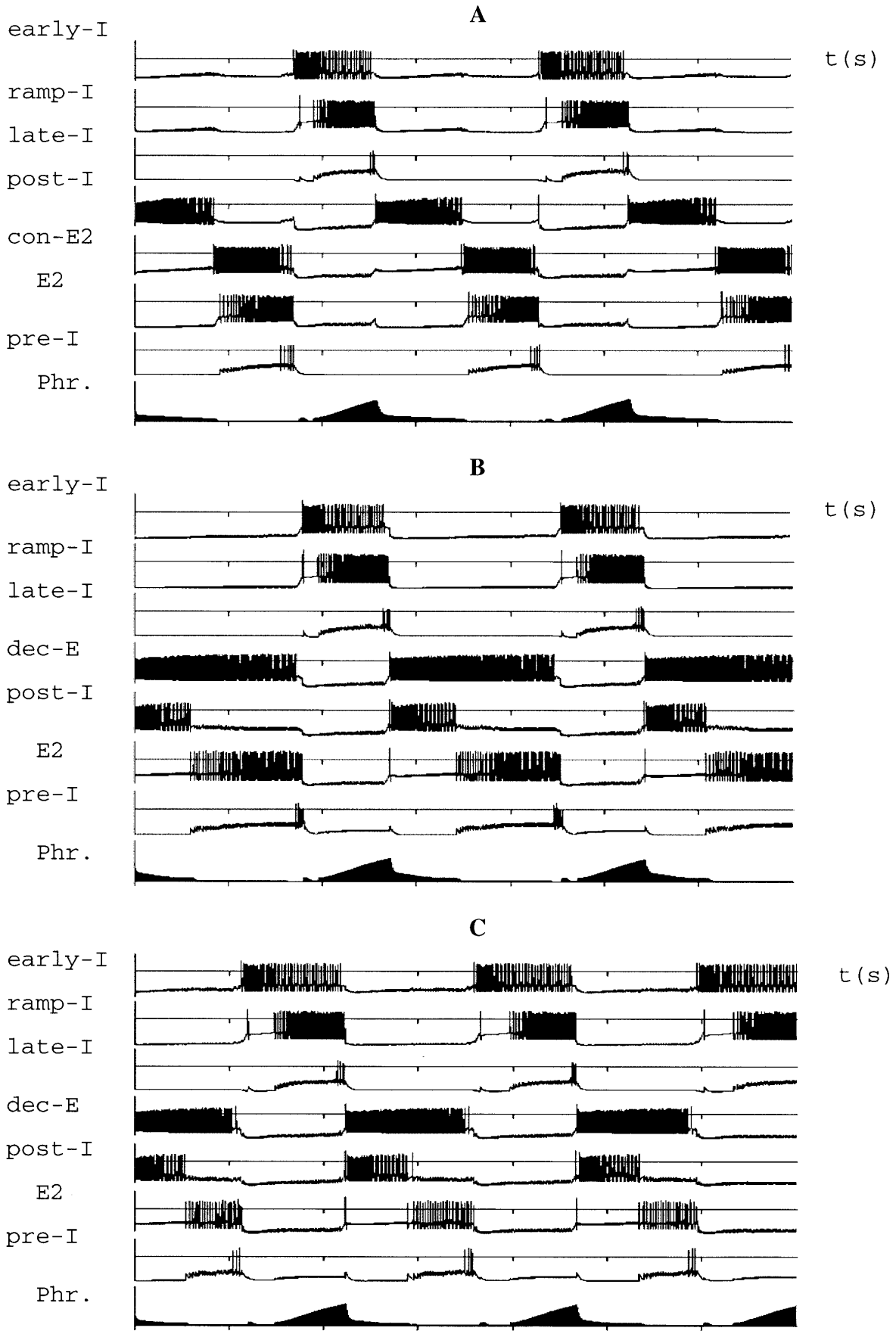

FIG. 3. Model performances under normal conditions. *A*: model 1; *B*: model 2; *C*: model 3.

or inhibitory) input to pre-I neurons was found in the literature, we arbitrarily set the tonic input synaptic weights in pre-I neurons to be negative and equal to the inhibitory input weights in late-I neurons (Rybak et al. 1997b).

In previous simulations, it was not necessary to distinguish the contribution of the CS drive from the total tonic drive to each respiratory neuron. In present study, we separated the CS input from the total drive to investigate the effects of CS nerve simulation on CRPG performance (see Figs. 1*B* and 2*C*). For this, we used the specific coefficients that defined the percentage of CS drive relative to the total drive to each respiratory neuron type (Tables 1–3).

SLN input to the respiratory network

In all our models, SLN afferents excite post-I neurons and inhibit all other expiratory neurons (E2, con-E2, dec-E; Figs. 1*B* and 2*C*). The excitatory SLN input to post-I neurons was described previously (Ogilvie et al. 1992; Remmers et al. 1986). The inhibitory inputs to E2, con-E2, and dec-E neurons are based on the data that SLN stimulation provides inhibition or hyperpolarization of expiratory neurons (Ballantyne and Richter 1986; Jiang and Lipski 1992; Ogilvie et al. 1992). The synaptic weights of SLN input to the above neurons used in models 1–3 are shown in Tables 1–3, respectively.

Stimuli used in model experiments

The single square pulses of constant amplitude and 200–300 ms in duration applied to SLN, vagus or CS nerves (see Figs. 1*B* and 2*C*) were used in our model experiments to simulate short-duration (phasic) electrical stimulation of corresponding nerves. The same square pulses applied to the input of the ''lung'' module (Figs. 1*B* and 2*C*) produced changes in the lung volume and were used to simulate lung inflation. The continuous stimuli of constant magnitude applied to the different nerves simulated a maintained electrical stimulation. The amplitudes of short-duration stimuli and the magnitudes of continuous stimulation were estimated as relative values in respect to the total tonic drive to the respiratory network, $I_o = 1$. The amplitude of stimuli producing an increase in lung volume (''lung inflation'') was estimated as a relative value in respect to the maximal lung volume, $L_{max} = 1$.

RESULTS

Model performances during SLN stimulation

The effects of short SLN stimulation on model performances were studied using 200-ms pulse stimuli of different amplitudes applied to SLN input (Figs. 1*B* and 2*C*). Stimuli of relatively small amplitude did not cause a phase singularity in the respiratory rhythm generated by any model. The effects of intermediate and strong SLN stimuli on models 1–3 are shown in Figs. 4, *A* and *B*, 5, *A* and *B*, and 6, *A* and *B*, respectively. In all models, the medium amplitude stimuli caused a phase singularity (early onset of the next inspiration) only when they were applied at the end of expiration (in Figs. 4*A*, 5*A*, and 6*A*, only the 3rd of 3 stimuli delivered at the end of expiration provides phase resetting). Stronger stimuli applied in any phase of the respiratory cycle caused a transition to inspiration (Figs. 4*B*, 5*B*, and 6*B*).

The performances of models 1–3 during maintained SLN

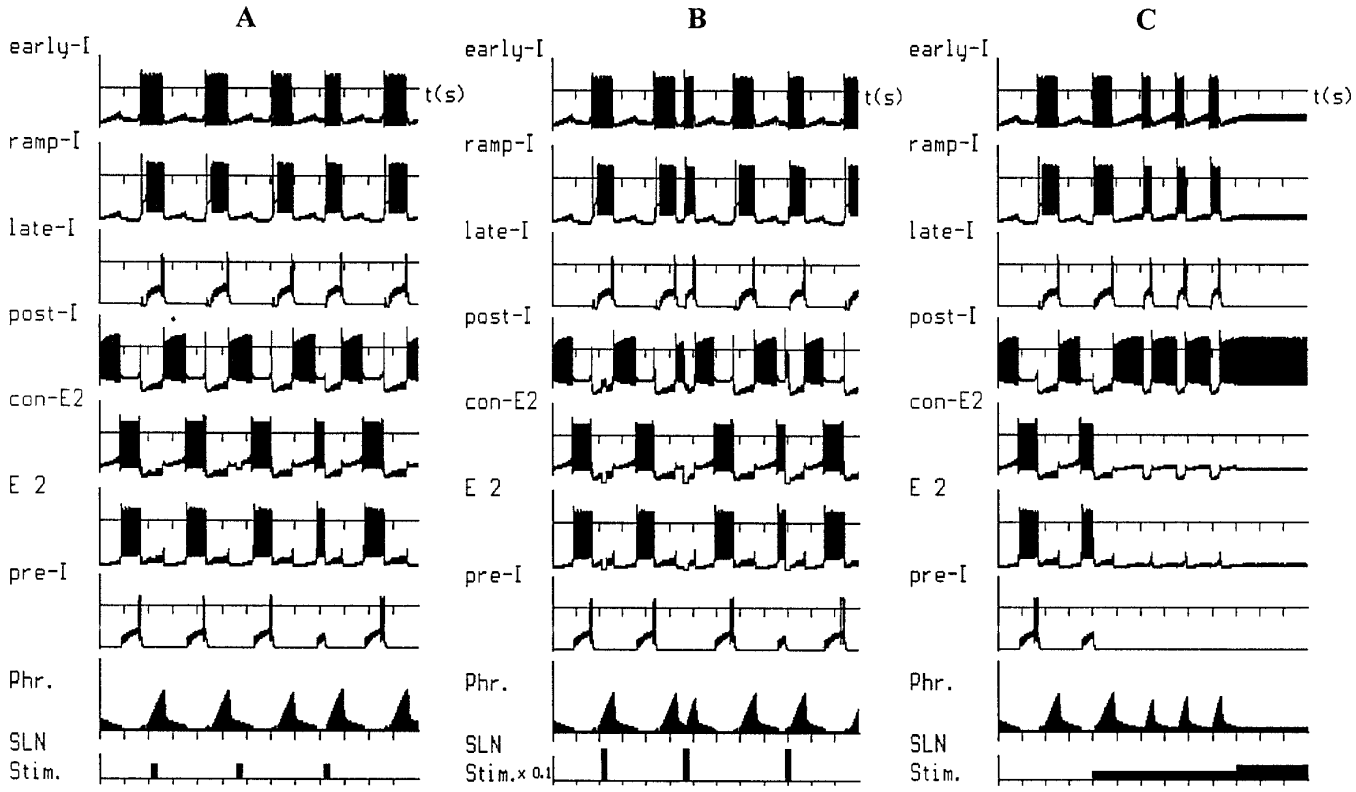

FIG. 4. Performance of model 1 during superior laryngeal (SLN) stimulation of different types. *A*: short-duration (200 ms), medium amplitude ($I_{sVLN} = 0.8 \cdot I_o = 0.8$) stimulus applied during different phases of respiratory cycle. *B*: short-duration strong stimulus (200 ms; $I_{sVLN} = 2.0$) delivered during different phases of respiratory cycle. *C*: sustained stimulation ($I_{sVLN} = 0.4$ and $I_{sVLN} = 0.8$).

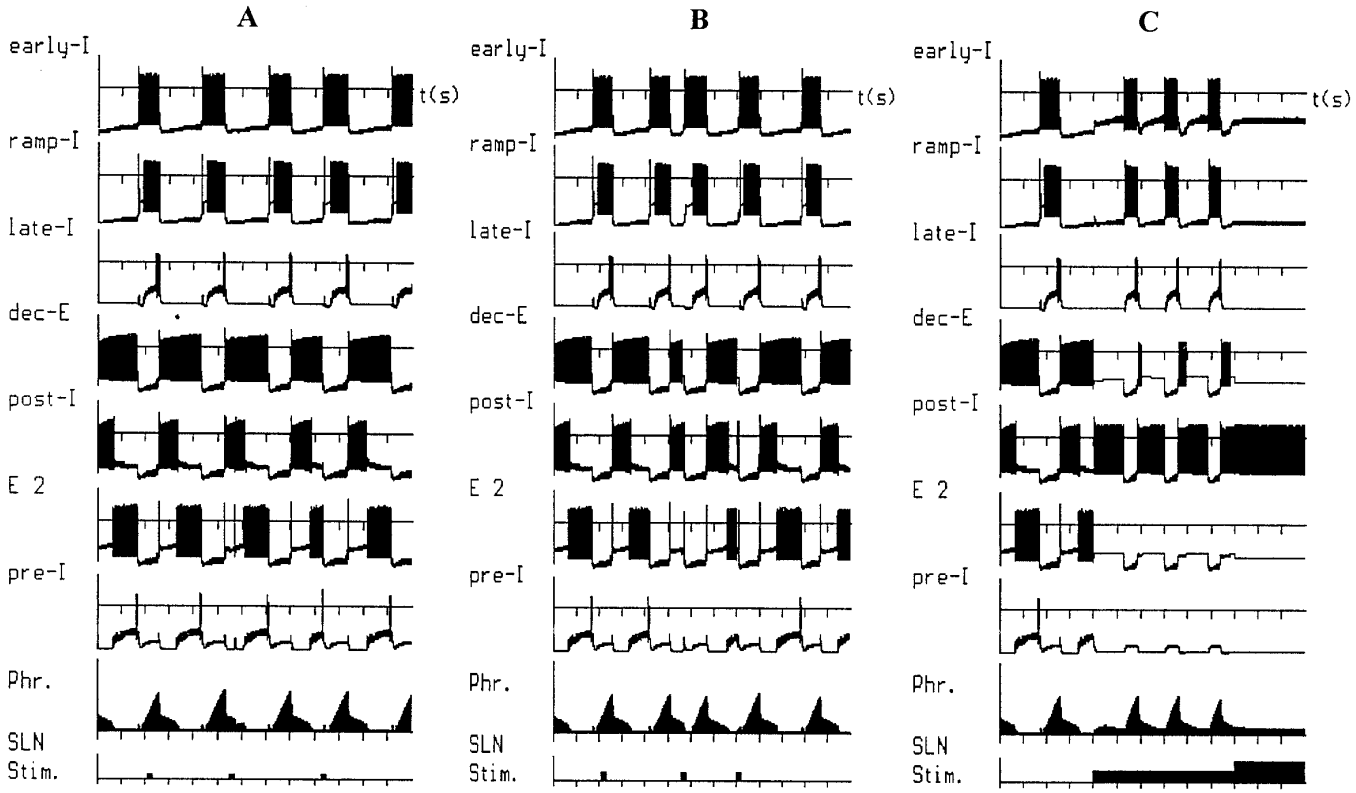

FIG. 5. Performance of model 2 during SLN stimulation of different types. *A*: short-duration (200 ms) medium amplitude stimulus ($I_{sVLN} = 0.2 \cdot I_o = 0.2$) applied during different phases of respiratory cycle. *B*: short-duration strong stimulus (200 ms; $I_{sVLN} = 0.4$) delivered during different phases of respiratory cycle. *C*: sustained stimulation ($I_{sVLN} = 0.6$ and $I_{sVLN} = 1.2$).

stimulation are shown in Figs. 4*C*, 5*C*, and 6*C*, respectively. In all models, relatively weak sustained stimulation produced a two-phase rhythm comprising inspiration and postinspiration (see *middle* in Figs. 4*C*, 5*C*, and 6*C*). In all models, a stronger sustained SLN stimulation produced a cessation of respiratory oscillations in the postinspiratory phase (i.e., ''postinspiratory apnea''; see *right* in Figs. 4*C*, 5*C*, and 6*C*).

Model performances during vagus nerve stimulation and lung inflation

The effects of short electrical stimulation of the vagus nerve were studied using 200-ms stimuli of different amplitudes applied to the vagas nerve input (Figs. 1*B* and 2*C*). Depending on their amplitude and phase, these stimuli terminated inspiration. Our simulations showed that the threshold for inspiratory termination decreased during the course of the inspiratory phase with approximately hyperbolic dependence in all three models. The effects of short-duration vagus nerve stimulation applied during inspiration on the performances of models 1–3 are shown in Figs. 7*A*, 8*A*, and 9*A*, respectively. In each figure, three stimuli are given. The first stimulus of large amplitude applied at the beginning of inspiration terminates inspiration. The second stimulus, which has a smaller amplitude but is applied at the same phase, does not terminate inspiration. The third stimulus has the same amplitude as the second stimulus, but is delivered at a later phase of inspiration terminates this inspiration.

To study a dynamic effect of sustained vagal stimulus on threshold for inspiratory termination we used the experimental protocol of Younes and Polacheck (1981). The conditioning stimulus with an amplitude less than the inspiratory off-switch threshold was applied to the vagus nerve. Then, a 200-ms pulse stimulus was used to test the dynamic changes of threshold. We found that effectiveness of the conditioning stimulus increased progressively and declined thereafter.

A 200-ms pulse of lung volume was used in our model experiments to simulate a short-term lung inflation. These stimuli (lung volume pulses) were applied at different times during expiration and produced different effects on the respiratory pattern in models 1–3 (Figs. 7*B*, 8*B*, and 9*B*).

In model 1, stimuli delivered in the postinspiratory phase prolonged this phase and the entire expiratory interval (the 1st stimulus in Fig. 7*B*). This prolongation was larger when stimuli were applied later in the postinspiratory phase. However, the same stimuli applied in the late expiratory (stage II) phase did not affect the expiratory duration (the 2nd stimulus in Fig. 7*B*). The entire late expiratory phase was insensitive to lung inflation.

In model 2, stimuli delivered at any time during expiration (postinspiratory or late expiratory phase) prolonged expiration (Fig. 8*B*). The prolongation was larger when the stimulus was applied later in the expiratory interval. The maximal prolongation occurred when the stimulus was delivered just before the time of expected termination of expiration (the 3rd stimulus in Fig. 8*B*).

Behavior of model 3 was similar to model 2. Stimuli

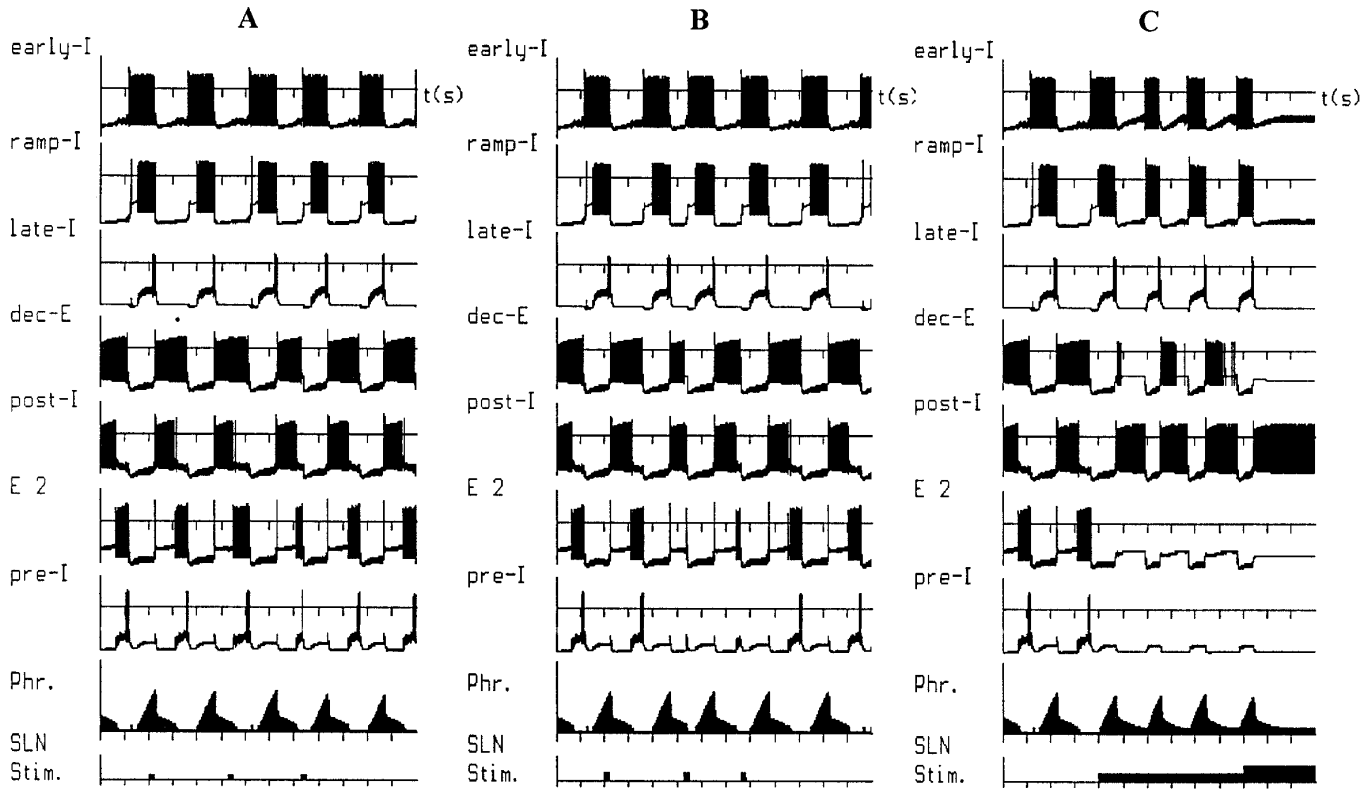

FIG. 6. Performance of model 3 during SLN stimulation of different types. *A*: short-duration (200 ms) medium amplitude stimulus ($I_{sVLN} = 0.2 \cdot I_o = 0.2$) applied during different phases of respiratory cycle. *B*: short-duration strong stimulus (200 ms; $I_{sVLN} = 0.4$) delivered during different phases of respiratory cycle. *C*: sustained stimulation ($I_{sVLN} = 0.5$ and $I_{sVLN} = 1.0$).

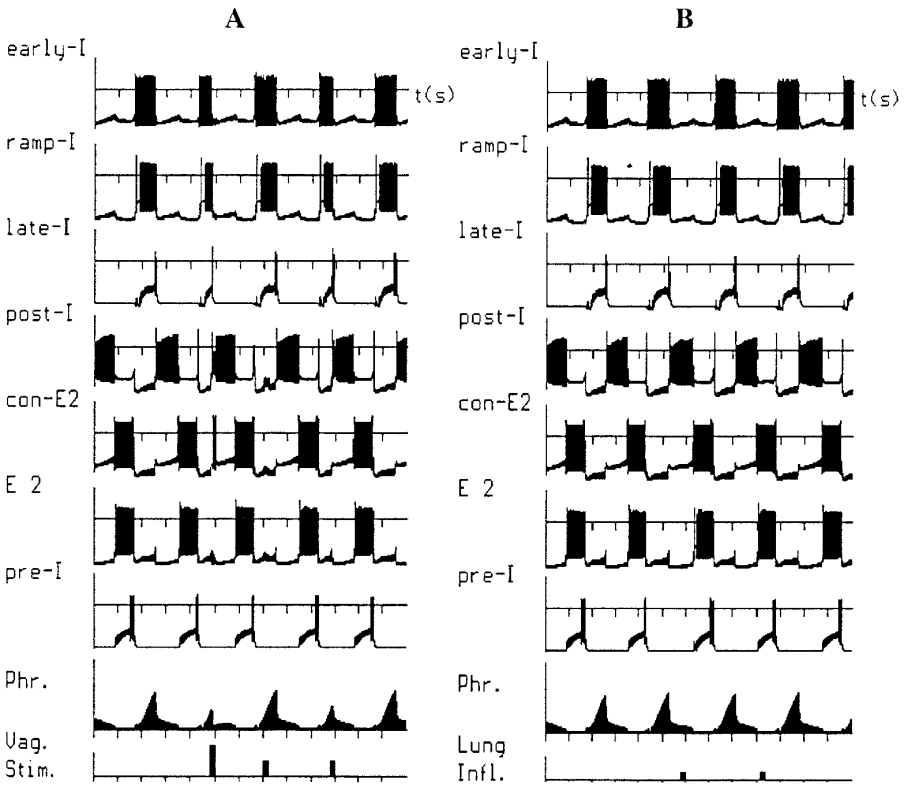

FIG. 7. Performance of model 1 during vagus nerve stimulation and lung inflation. *A*: short-duration (200 ms) large ($I_{sVag} = 2.0 \cdot I_o = 2.0$) and medium amplitude ($I_{sVag} = 1.0$) stimuli applied to vagus nerve at different times during inspiration. *B*: short-term increase in lung volume (200 ms; $I_{sL} = 0.4 \cdot L_{max} = 0.4$) applied at different times during expiration.

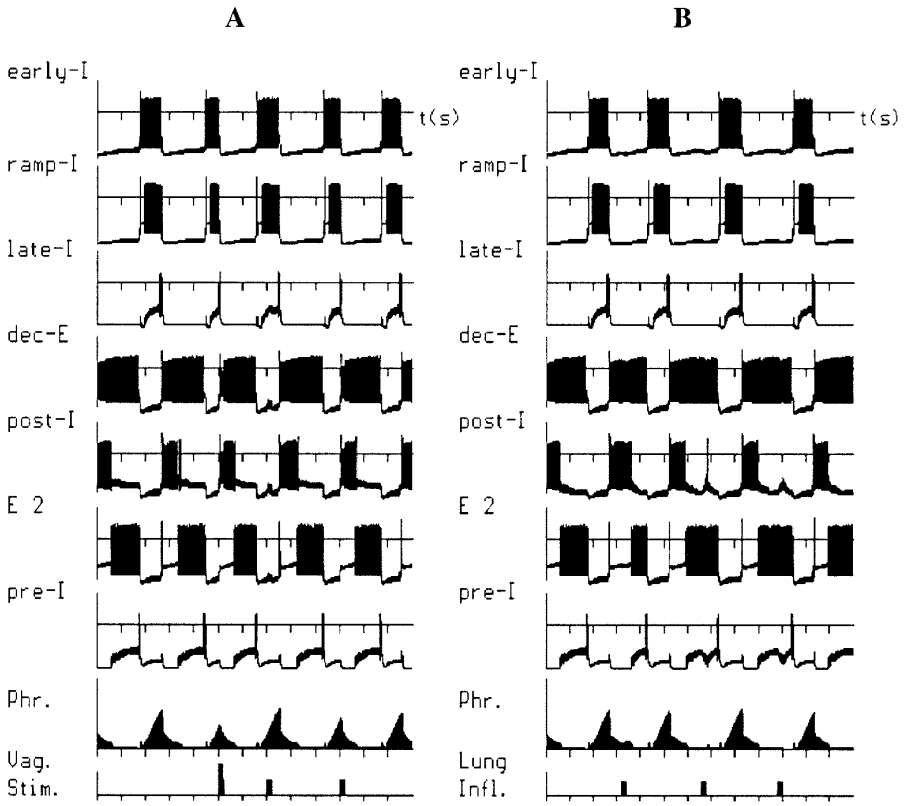

FIG. 8. Performance of model 2 during vagus nerve stimulation and lung inflation. *A*: short-duration (200 ms) large amplitude ($I_{sVag} = 2.0 \cdot I_o = 2.0$) and medium amplitude ($I_{sVag} = 1.0$) stimuli applied to vagus nerve at different times during inspiration. *B*: short-term increase in lung volume (200 ms; $I_{sL} = 0.8 \cdot L_{max} = 0.8$) applied at different times during expiration.

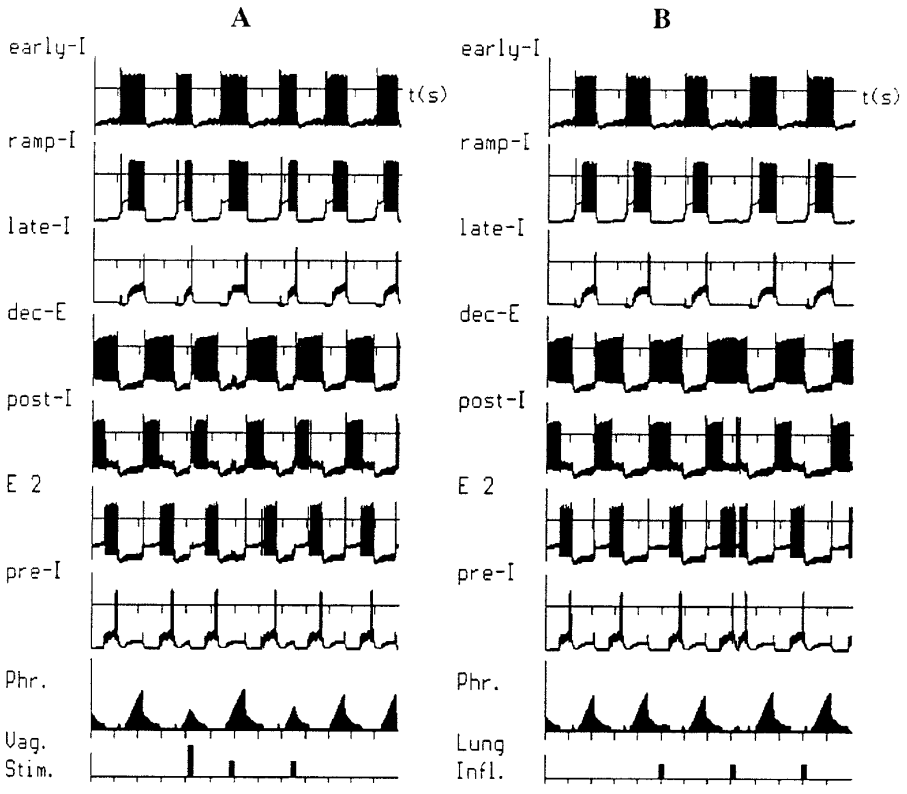

FIG. 9. Performance of model 3 during vagus nerve stimulation and lung inflation. *A*: short-duration (200 ms) large amplitude ($I_{sVag} = 2.2 \cdot I_o = 2.2$) and medium amplitude ($I_{sVag} = 1.1$) stimuli applied to vagus nerve at different times during inspiration. *B*: short-term increase in lung volume (200 ms; $I_{sL} = 0.8 \cdot L_{max} = 0.8$) applied at different times during expiration.

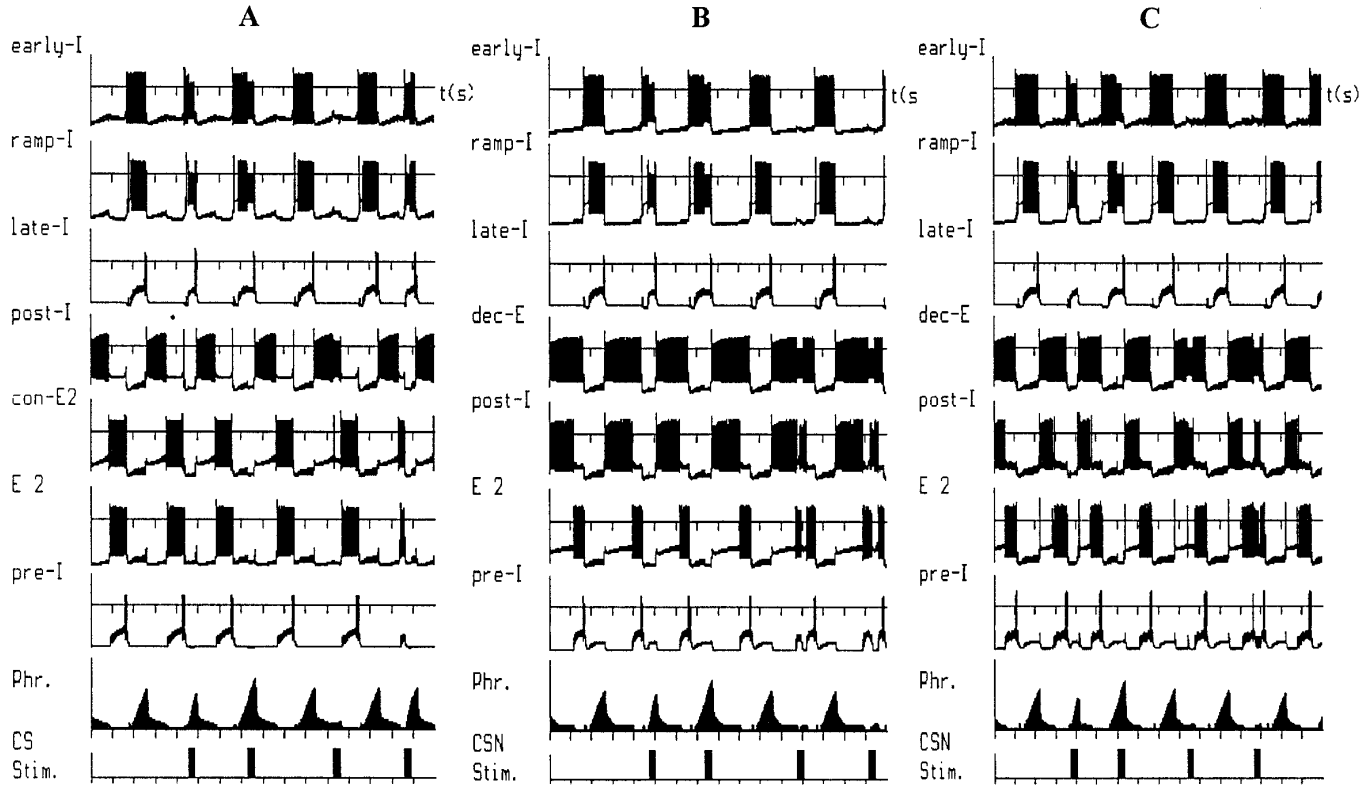

FIG. 10. Model performances during short-duration stimulation (300 ms; $I_{sVag} = 1.7 \cdot I_o = 1.7$) applied to carotid sinus (CS) nerve during different phases of respiratory cycle: model 1 (*A*); model 2 (*B*); model 3 (*C*).

delivered in expiration also prolonged this expiration (Fig. 9*B*). However, there was a short period at the very end of expiration (~200-ms before the expected expiratory termination), which was insensitive to stimulation (the 3rd stimulus in Fig. 9*B*).

Sustained stimulation of the vagus nerve stopped respiratory oscillations in the postinspiratory phase (''postinspiratory apnea'') in all three models.

Model performances during CS nerve stimulation

The performance of models 1–3 during phasic stimulation of the CS nerve by 300 ms stimuli are shown in Fig. 10, *A–C*, respectively. In all three models, stimuli delivered at the beginning of the inspiratory phase caused a shortening of the inspiratory phase (the 1st stimuli in Fig. 10, *A–C*) whereas stimuli applied in the middle or at the end of the inspiratory phase prolonged the phase and caused an increase in the amplitude of the phrenic burst (the 2nd stimuli in Fig. 10, *A–C*). Stimuli delivered in the postinspiratory phase caused a prolongation of expiration (the 3rd stimuli in Fig. 10, *A–C*).

The behavior of the models were different when the stimuli were delivered during the late expiratory phase. In model 1, these stimuli were either ineffective or caused an early onset of the next inspiration and a shortening of the current expiration (4th stimulus in Fig. 10*A*). Alternatively, in models 2 and 3, these stimuli caused a prolongation of the expiratory interval (4th stimulus in Fig. 10, *B* and *C*). We were unable to find any parameters of CS input in these models; this could provide opposite changes in the duration of the expiratory interval when CS stimuli were applied in postinspiration versus late expiration.

DISCUSSION

The objective of this study was to make a comparative analysis of different CRPG models by their performances during stimulation of different respiratory afferents. Because CRPG models studied employ different mechanisms for ramp firing of the E2 neurons and for expiratory off-switching, their responses to various stimulations differed mostly during the late (stage II) expiratory phase.

Effects of SLN stimulation

All our CRPG models demonstrated the following phase resetting behavior in response to short-duration SLN stimuli: weak stimuli had no effect on the respiratory rhythm; stimuli of medium amplitude caused a resetting of the respiratory cycle (phase singularity) at the end of expiration; and strong stimuli applied in any phase reset the respiratory cycle to inspiration. This phase resetting behavior is consistent with the data obtained by Paydarfar et al. (1986) in studies of phase-resetting effects of short-duration electrical SLN stimulation on the respiratory pattern in cat.

All models showed a two-phase respiratory rhythm comprising inspiration and postinspiration during relatively weak, sustained SLN stimulation; this is consistent with experimental results of Remmers et al. (1986). All models

demonstrated a ''postinspiratory apnea'' in response to stronger SLN stimulation, corresponding to the observations of Lawson (1981) and Remmers et al. (1986).

Thus all models displayed similar and physiologically plausible changes in the respiratory pattern during SLN stimulation of different types.

Effects of vagotomy, vagus nerve stimulation, and lung inflation

Earlier we found that disconnection of PSR feedback in all our models caused an increase in the amplitude and duration of ramp-I activity and phrenic discharges (Rybak et al. 1997b). This is consistent with experimental data (Cohen 1979; Feldman 1986; von Euler 1986) and apparently reflects the loss of the Hering-Breuer inspiration-inhibiting reflex. In all models, loss of feedback reduced the duration of post-I neuron activity and the postinspiratory phase, which corresponds to the conclusion of Richter et al. (1986).

On the other hand, the models showed different changes in the duration of the late expiratory (stage II) phase and the entire expiratory interval when PSR feedback was disconnected (Rybak et al. 1997b). In model 1, the duration of late expiration did not change whereas the entire expiratory duration decreased due to the shortening of the postinspiratory phase. This is consistent with data presented by Richter et al. (1986) and may reflect the loss of the Hering-Breuer expiration-facilitating reflex (Cohen 1979; Feldman 1986; von Euler 1986). Alternatively, in our other models (3-phase models 2 and 3 and both 2-phase models), the duration of expiration increased following the increase in duration of the preceding inspiration. This corresponds to the conclusion of Clark and von Euler (1972) about a maintained relationship between the durations of inspiration (T_I) and expiration (T_E). However, it has been shown that the coupling of T_I and T_E in vivo is restricted to a limited set of circumstances (Mitchell et al. 1982) and hence may not be supportive evidence favoring one model over another.

In all models, a short-duration stimulus applied to the vagus nerve during inspiration terminated this phase if the stimulus amplitude exceeded some threshold. The threshold for inspiratory termination decreased during the course of the inspiratory phase with approximately hyperbolic dependence, which is consistent with experimental data (Boyd and Maaske 1939; Clark and von Euler 1972; Cohen 1979; Gautier et al. 1981; Larrabee and Hodes 1948; von Euler 1986). The hyperbolic decrease in the threshold for inspiratory termination results from slow depolarization in the late-I neuron during inspiration, which, in turn, is provided by both increasing excitation from the ramp-I neuron and decreasing inhibition from the early-I neuron. The decrease in the early-I neuron activity results from two factors: adaptive properties of this neuron and volume-dependent PSR feedback, which inhibits this neuron. The first factor is independent of phasic PSR feedback and produces dynamic alteration of inspiratory off-switch threshold in response to vagal inputs. The dynamic nature of threshold for inspiratory termination was elucidated by Younes and Polacheck (1981). Our model showed dynamic changes in the threshold similar to those described by Younes and Polacheck: effectiveness of the constant conditioning stimulus applied to the vagal input increased progressively and declined thereafter. Thus the dynamic effect discovered by Younes and Polacheck may result partly from the adaptive properties of early-I neurons.

A short-duration increase in lung volume (''lung inflation'') applied at the beginning of the expiratory interval prolonged expiration in all models. This is consistent with experimental data by Bradley (1976) and Knox (1973).

Behavior of the models was different when these stimuli were delivered during the late (stage II) expiratory phase. In model 1, the entire late expiratory phase was insensitive to lung inflation. In contrast, no insensitive period was found in model 2 (or in either of our 2-phase models): a pulse of lung volume applied at any time during expiration prolonged the expiatory interval. A period insensitive to lung inflation was found in model 3, but it was restricted to the end of expiration.

The literature concerning the effects of vagus nerve stimulation during the late part of expiration on the respiratory pattern are contradictory. For example, Sammon et al. (1993) concluded that stimulation of the vagus nerve after midexpiration evoked unpredictable responses including a prolongation or shortening of the expiratory duration. Remmers et al. (1986) found that stimulation of PSR during stage II of expiration did not influence expiratory duration; this is consistent with model 1. However, Bradley (1976) used electrical stimulation of vagus nerve and did not find any insensitive period at the end of expiration; this corresponds to our model 2. In contrast, Knox (1973) and Feldman and Gautier (1976) found that the last 400 ms of the expiratory interval were insensitive to vagus nerve stimulation. It is not clear whether these data correspond to the results of Remmers et al. (1986), since the insensitive periods found by Knox (1973) and Feldman and Gautier (1976) were probably shorter than the duration of the late (stage II) expiratory phase. The behavior of model 3 is most consistent with Knox's (1973) data. The differences in experimental data concerning effects of vagal stimulation during expiration may result from different experimental conditions and methods of stimulation. For example, Knox (1973) used a sudden lung inflation whereas Bradley (1976) and Sammon et al. (1993) employed electrical stimulation of the vagus nerve. This inconsistency in experimental data makes it difficult to compare the models and assess model plausibility, but model 1 appears to be most closely matched to experimental data.

Sustained vagus nerve stimulation in all models stopped respiratory oscillation in the postinspiratory phase (postinspiratory apnea); this is consistent with Remmers et al. (1986).

Effects of CS nerve stimulation

Phasic CS stimulation in all models evoked the following effects: stimuli delivered at the beginning of inspiration shortened this phase, stimuli applied in the middle or at the end of inspiration prolonged it and increased the amplitude of phrenic bursts, and stimuli delivered in the first half of expiration (postinspiratory phase) prolonged expiration. All these modeling results are consistent with the experimental findings of Eldridge (1972, 1976). In addition, the effect of

CS stimulation during the postinspiratory phase on model performances is consistent with Remmers et al. (1986) results. However, model 1 was the only model that demonstrated a shortening of expiration when CS stimuli were delivered in the late expiratory phase; this corresponds to Eldridge's (1972, 1976) and Remmers et al.'s (1986) data. Moreover, the reversal-type dependence between the duration of expiration and time of stimulus presentation in model 1 was qualitatively similar to that drawn from Remmers' experiments (see Fig. 8*A* in Remmers et al. 1986). In contrast to model 1, all other our models (models 2 and 3 and 2-phase models) responded to stimuli applied during the late (stage II) expiratory phase with a prolongation of expiration. We could not find any set of parameters for CS input in these models that replicated the reversal effects of CS nerve stimulation on expiratory duration when stimuli were delivered during I versus II stage of expiration as described by Eldridge (1972, 1976) and Remmers et al. (1986). Thus our model experiments with CS nerve stimulation also suggest that model 1 is more realistic than the other models.

In conclusion, our CRPG models demonstrate a number of plausible (consistent with experimental data) alterations of the central respiratory pattern during different perturbations applied to respiratory afferent nerves. We consider this as additional evidence supporting the viability of our CRPG models. Considering all our simulation results, we suggest that model 1 is more plausible than the other models. Taking into account the differences between model 1 and the other models we suggest that the concept of respiratory rhythmogenesis based on the essential role of post-I neurons is probably more plausible than the concept employing specific properties of dec-E neurons and that the ramp firing patterns in E2 neurons probably reflects intrinsic membrane properties rather than disinhibition from dec-E neurons. However, further experimental studies and simulations are required to further test CRPG models based on different proposed neural mechanisms.

The authors are grateful to J. Champagnat, Y. Fuentes, J. Hopfield, K. F. Morris, B. A. Ogunnaike, M. Pottmann, and R. F. Rogers for useful discussion of the models.

This research was supported by National Science Foundation Grant BIR93-153-03, Air Force Grant F49620-93-1-0285, and E. I. du Pont de Nemours. J.F.R. Paton holds a British Heart Foundation Lectureship.

Address reprint requests to I. A. Rybak.

Received 8 April 1996; accepted in final form 12 December 1996.

REFERENCES

BALLANTYNE, D. AND RICHTER, D. W. The non-uniform character of expiratory synaptic activity in expiratory bulbospinal neurons of the cat. *J. Physiol. Lond.* 370: 433–456, 1986.

BOTROS, S. M. AND BRUCE, E. N. Neural network implementation of the three-phase model of respiratory rhythm generation. *Biol. Cybern.* 63: 143–153, 1990.

BRADLEY, G. W. The effect of CO_2, body temperature and anesthesia on the response to vagal stimulation. In: *Respiratory Centers and Afferent Systems*, edited by B. Duron. Paris: INSERM, 1976, p. 139–154.

BOYD, T. E. AND MAASKE, C. A. Vagal inhibition of inspiration and accompanying changes of respiratory rhythm. *J. Neurophysiol.* 2: 533–542, 1939.

CLARK, F. J. AND VON EULER, C. On the regulation of depth and rate of breathing. *J. Physiol. Lond.* 222: 267–295, 1972.

COHEN, M. I. Neurogenesis of respiratory rhythm in the mammal. *Physiol. Rev*. 59: 1105–1173, 1979.

COHEN, M. I. AND FELDMAN, J. L. Models of respiratory phase-switching. *Federation Proc.* 36: 2367–2374, 1977.

DUFFIN, J. A model of respiratory rhythm generation. *Neuroreport* 2: 623–626, 1991.

DUFFIN, J., EZURE, K., AND LIPSKI, J. Breathing rhythm generation: focus on rostral ventrolateral medulla. *News Physiol. Sci.* 10: 133–140, 1995.

ELDRIDGE, F. L. The importance of timing on the respiratory effects of intermittent carotid sinus nerve stimulation. *J. Physiol. Lond.* 222: 297–318, 1972.

ELDRIDGE, F. L. Expiratory effects of brief carotid sinus nerve and carotid body stimulations. *Respir. Physiol.* 26: 395–410, 1976.

EZURE, K. Synaptic connections between medullary respiratory neurons and consideration on the genesis of respiratory rhythm. *Prog. Neurobiol.* 35: 429–450, 1990.

FELDMAN, J. L. Neurophysiology of breathing in mammals. In: *Handbook of Physiology. The Nervous System. Intrinsic Regulatory Systems of the Brain.* Bethesda, MD: Am. Physiol. Soc., 1986, sect. 1, part IV, p. 463–524.

FELDMAN, J. L. AND GAUTIER, H. Interaction of pulmonary afferents and pneumotaxic center in control of respiratory pattern in cats. *J. Neurophysiol.* 39: 31–44, 1976.

GAUTIER, H., BONORA, M., AND GAUDY, J. N. Breuer-Hering inflation reflex and breathing pattern in anesthetized humans and cats. *J. Appl. Physiol.* 51: 1162–1168, 1981.

GEMAN, S. AND MILLER, M. Computer simulation of brainstem respiratory activity. *J. Appl. Physiol.* 41: 931–938, 1976.

GOTTSCHALK, A., OGILVIE, M. D., RICHTER, D. W., AND PACK, A. I. Computational aspects of the respiratory pattern generator. *Neural Comput.* 6: 56–68, 1994.

JIANG, C. AND LIPSKI, J. Synaptic inputs to medullary respiratory neurons from superior laryngeal afferents in the cat. *Brain Res.* 584: 197–206, 1992.

KLAGES, S., BELLINGHAM, M. C., AND RICHTER, D. W. Late expiratory inhibition of stage 2 expiratory neurons in the cat—a correlate of expiratory termination. *J. Physiol. Lond.* 70: 1307–1315, 1993.

KNOX, C. K. Characteristics of inflation and deinflation reflexes during expiration in the cat. *J. Neurophysiol.* 36: 284–295, 1973.

LARRABEE, M. G. AND HODES, R. Cyclic change in the respiratory centers, revealed by effects of afferent impulses. *Am. J. Physiol.* 155: 147–164, 1948.

LAWSON, E. E. Prolonged central respiratory inhibition following reflex-induced apnea. *J. Appl. Physiol.* 50: 844–879, 1981.

LAWSON, E. E., RICHTER, D. W., BALLANTYNE, D., AND LALLEY, P. M. Peripheral chemoreceptor inputs to medullary inspiratory and postinspiratory neurons of cat. *Pfluegers Arch.* 414: 523–433, 1989.

MITCHELL, G. S., CROSS, B. A., HIRAMOTO, T., AND SCHELD, P. Interactions between lung stretch and Pa_{CO2} in modulating ventilatory activity in dogs. *J. Appl. Physiol.* 53: 185–191, 1982.

OGILVIE, M. D., GOTTSCHALK, A., ANDERS, K., RICHTER, D. W., AND PACK, A. I. A network model of respiratory rhythmogenesis. *Am. J. Physiol.* 263 (*Regulatory Integrative Comp. Physiol.* 31): R962–R975, 1992.

PAYDARFAR, D., ELDRIDGE, F. L., AND KILEY, J. P. Resetting of mammalian respiratory rhythm: existence of a phase singularity. *Am. J. Physiol.* 250 (*Regulatory Integrative Comp. Physiol.* 19): R721–R727, 1986.

REMMERS, J. E., RICHTER, D. W., BALLANTYNE, D., BAINTON, C. R., AND KLEIN, J. P. Reflex prolongation of stage I of expiration. *Pfluegers Arch.* 407: 190–198, 1986.

RICHTER, D. W. AND BALLANTYNE, D. A three phase theory about the basic respiratory pattern generator. In: *Central Neurone Environment,* edited by M. Schla f ke, H. Koepchen, and W. See. Berlin: Springer, 1983, p. 164–174.

RICHTER, D., BALLANTYNE, D., AND REMMERS, J. E. How is the respiratory rhythm generated? A model. *News Physiol. Sci*. 1: 109–112, 1986.

RICHTER, D., BALLANTYNE, D., AND REMMERS, J. E. The different organization of medullary post- inspiratory activities. *Pfluegers Arch.* 410: 420–427, 1987.

RICHTER, D. W. Neural regulation of respiration: rhythmogenesis and afferent control. In: *Comprehensive Human Physiology,* edited by R. Greger and U. Windhorst. Berlin: Springer-Verlag, 1996, vol. II, p. 2079–2095.

RUBIO, J. E. A new mathematical model of the respiratory center. *Bull. Math. Biophys*. 34: 467–481, 1972.

RYBAK, I. A., PATON, J.F.R., AND SCHWABER, J. S. Modeling neural mecha-

nisms for genesis of respiratory rhythm and pattern. I. Models of respiratory neurons. *J. Neurophysiol.* 77: 1994–2006, 1997a.

RYBAK, I. A., PATON, J.F.R., AND SCHWABER, J. S. Modeling neural mechanisms for genesis of respiratory rhythm and pattern. II. Network models of the central respiratory pattern generator. *J. Neurophysiol.* 77: 2007–2026, 1997b.

SAMMON, M., ROMANIUK, J. R., AND BRUCE, E. N. Bifurcations of the respiratory pattern produced with phasic vagal stimulation in the rat. *J. Appl. Physiol.* 75: 912–926, 1993.

SCHWARZACHER, S. W., WILHEM, Z., ANDERS, K., AND RICHTER, D. W. The medullary respiratory network in the rat. *J. Physiol. Lond.* 435: 631–644, 1991.

VON EULER, C. Brainstem mechanism for generation and control of breathing pattern. In: *Handbook of Physiology. The Respiratory System. Control of Breathing*. Washington, DC: Am. Physiol. Soc., 1986, sect. 3., vol. II, p. 1–67.

YOUNES, M. K. AND POLACHECK, J. Temporal changes in effectiveness of a constant inspiratory-terminating vagal stimulus. *J. Appl. Physiol.* 50: 1183–1192, 1981.